Theoretical Surface Spectroscopy of NO on the Pt(111) Surface with the DAM (Dipped Adcluster Model) and the SAC-CI (Symmetry-Adapted-Cluster Configuration-Interaction) Method

Hiroshi Nakatsuji, Norihiko Matsumune, and Kei Kuramoto

Department of Synthetic Chemistry and Biological Chemistry, Graduate School of Engineering, Kyoto University, Nishikyo, Kyoto 615-8510, Japan, and Fukui Institute for Fundamental Chemistry, Kyoto University, Sakyo, Kyoto 606-8103, Japan

JCTC Journal of Chemical Theory and Computation

Reprinted from
Volume 1, Number 2, Pages 239–247

JCTC Journal of Chemical Theory and Computation

Theoretical Surface Spectroscopy of NO on the Pt(111) Surface with the DAM (Dipped Adcluster Model) and the SAC-CI (Symmetry-Adapted-Cluster Configuration-Interaction) Method

Hiroshi Nakatsuji,*,†,‡ Norihiko Matsumune,† and Kei Kuramoto†

Department of Synthetic Chemistry and Biological Chemistry, Graduate School of Engineering, Kyoto University, Nishikyo, Kyoto 615-8510, Japan, and Fukui Institute for Fundamental Chemistry, Kyoto University, Sakyo, Kyoto 606-8103, Japan

Received September 20, 2004

Abstract: Theoretical surface spectroscopy for NO on the Pt(111) surface is carried out and combined with the experimentally known facts to elucidate the structures, absorption sites, absorption energies and K-shell binding energies of NO adsorbates on the surface. The electronic structures were studied by using the dipped adcluster model (DAM) for chemisorptions on a metal surface proposed previously and the symmetry-adapted-cluster configuration-interaction (SAC-CI) method, which is an established method for studying molecular spectroscopy. The natures of the two different adsorption species suggested experimentally have clearly been identified based on the studies on the geometries, vibrational frequencies, adsorption energies, and the N and O K-shell binding energies. The PES (potential energy surface) of NO on the metal surface was also calculated. The most stable adsorption species was on the fcc or the hcp hollow site, and the on-top one was less stable. The 2-fold bridge site did not have a minimum on the PES and therefore was only transient. The inter NO interactions at higher densities were shown to be rather weak. We examined the cluster model (CM) vs the DAM as a model of the surface adsorption on a metal surface. The CM was shown to be unable to describe the adsorption of NO on a metal surface, demonstrating the importance of the electron transfer between the NO and Pt surfaces included in the DAM. The DAM and the SAC-CI methods proved to be a useful tool for studying the nature, electronic structure, and the spectroscopic properties of the adsorbates on a metal surface.

1. Introduction

Nitric oxides (NO_x) are the substances included in exhaust gases from automobiles, factories and industries. The nature of the adsorptions of NO_x on metal surfaces has been widely investigated by using spectroscopic techniques[1−15] such as electron energy loss spectroscopy (EELS), infrared reflection absorption spectroscopy (IRAS), scanning tunneling microscopy (STM), low-energy electron diffraction (LEED), electron spectroscopy for chemical analysis (ESCA), and ultraviolet(U) or X-ray(X) photoemission spectroscopy (PS). These experiments have given the information about the electronic structures and the bonding of the adsorbates on the metal surfaces. We investigate here the nature of the adsorptions of the simplest nitric oxide, NO on the Pt(111) surface.

There are many examples of molecular and dissociative adsorptions of NO on metal surfaces.[16] On a Pt surface, it is generally agreed that NO adsorbs molecularly at low temperature with its N atom toward the surface. Due to EELS[1,2,6,14] and IRAS[3,7,9,11] experiments, an N−O stretching band lay at the range of 1476−1516 cm^{-1} at low coverage,

* Corresponding author e-mail: hiroshi@sbchem.kyoto-u.ac.jp.
† Department of Synthetic Chemistry and Biological Chemistry, Kyoto University.
‡ Fukui Institute for Fundamental Chemistry, Kyoto University.

10.1021/ct049938z CCC: $30.25
Published on Web 01/29/2005

and as the coverage increased, a new band began to develop around 1700−1725 cm^{-1} and at the same time, the first band decreased: the first peak nearby 1500 cm^{-1} was converted into the new peak nearby 1700 cm^{-1}. Hayden[3] considered that NO converts from the bridge site to the on-top site at near-saturation coverage. Sexton et al.[2] also reported the existence of the two types of adsorbates at low and high coverage. Various adsorption models were suggested by many experimental techniques such as LEED[1,10,15] and STM.[13,14] Materer et al.[10] reported that an fcc hollow site adsorption was observed by the p(2 × 2) LEED pattern. Matsumoto et al.[15] also performed the dynamical LEED analysis and reported the adsorption sites of NO to be at the on-top site and at the fcc- and hcp-hollow sites.

The nature of the interaction between NO and a metal surface is interesting. NO is a radical in a gas phase and has one electron in the π^*-MO. When adsorbed on a metal surface, the NO stretching frequency shows a red shift from that of the gas phase: it is 1876 cm^{-1} in a gas phase and around 1500 cm^{-1} on Pt(111) at low coverage and is around 1600 cm^{-1} on Pd (111) at the same condition. This indicates that the electron transfer occurs on a metal surface from the metal surface to the adsorbate NO. Between the donation and the back-donation interactions between NO and a metal surface, the back-donation interaction is more important.

In the previous theoretical studies, Ge et al.[17] reported that the 3-fold fcc hollow site is most stable and the 3-fold hcp hollow site is next by the density functional theory (DFT) calculations using a cluster model. Koper et al.[18] compared the adsorption energies of the on-top and hollow sites by the DFT calculations and explained that the hollow site is more stable. Aizawa et al.[19] calculated the adsorption energies for the three types of coverage using the periodic boundary model. All of these reports show that the 3-fold hollow site is the most stable.

When NO is adsorbed on a Pt surface, electrons are withdrawn from the metal to NO. When we use the cluster model (CM), the effects of the free electrons of the bulk metal are not well described. We therefore use the dipped adcluster model (DAM)[20,21] proposed by one of the authors to describe the chemisorptions and catalytic reactions on a metal surface. It naturally describes the effect of the electron transfer between adsorbates and the metal surface and the image force effects characteristic to the metal surface. We study the structures, vibrations, absorption sites, and surface PES (potential energy surface) for the NO on the Pt(111) surface with the DAM combined with the density functional theory (DFT). We also study the possibility of the interadsorbate interactions expected at high coverage adsorptions.

The K-shell binding energies of NO adsorbates are observed experimentally and show some interesting features. Recently, we have shown that the SAC (symmetry adapted cluster)[22]/SAC-CI (configuration interaction)[23] method describes well the K-shell ionizations of various molecules in excellent agreement with the experimental values.[24] We apply here the SAC-CI method combined with the DAM to elucidate the origin of the different K-shell binding energies observed for NO at different coverage situations.

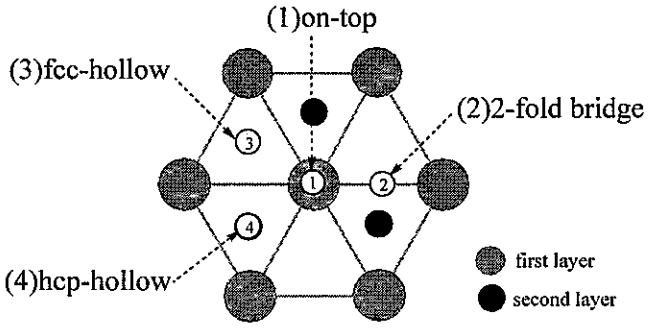

Figure 1. Model and four adsorption sites on the Pt(111) surface: (1) on-top, (2) 2-fold bridge, (3) 3-fold fcc-hollow, and (4) 3-fold hcp-hollow.

In all the aspects of the present study of the NO adsorbed on the Pt(111) surface, the importance of the DAM has been stressed. We then compare the DAM with the CM directly for the adsorption energy and some other properties of NO on the Pt(111) surface and then enter into the detailed discussions on the nature of the chemisorptions.

2. Computational Details

In this study, we used the DFT method with the B3LYP[25,26] potential and combined it with the dipped adcluster model (DAM).[20,21] The DAM was used to include the effect of the electron exchange between the adsorbates and the bulk metal, which is considered to be very important on the metal surface. The cluster model cannot describe such effect. We also included the energy correction due to the image force[27] on the metal surface. We used the highest spin-coupling model, and so one-electron transfer from the bulk metal to the adcluster was assumed.[20,21]

Four adsorption sites, (1) on-top, (2) 2-fold bridge, (3) 3-fold fcc-hollow, and (4) 3-fold hcp-hollow, shown in Figure 1, were investigated using the experimental geometry of the (111) surface. We used five different sizes of clusters shown in Figure 2 to mimic the (111) surface: (a) $Pt_3(3,0)$, (b) $Pt_4(4,0)$, and (c) $Pt_7(7,0)$ clusters, which contain respectively, three, four, and seven atoms only in the first layer, (d) $Pt_4(3,1)$ and (e) $Pt_{10}(7,3)$ clusters, which contain double layers.

The geometry of the adsorbed molecule on the surface was optimized using the DAM+DFT method. Materner et al. reported that the geometry relaxation of the metal−metal distance on the Pt(111) surface was very small; the change of the Pt−Pt bond length was less than 0.1 Å. Then, we used the fixed Pt−Pt bond length at its bulk lattice value of 2.77 Å.[28] The convergence criterion of the geometry optimization on the first derivative of the total energy was 0.0003 hartree/bohr (default value). After the optimizations, the vibrational analyses were carried out to evaluate the harmonic frequencies and the IR intensities.

All calculations were performed using the Gaussian 03 software package.[29] For the DFT calculations, the basis set for Pt atom was (3s3p3d)/[3s3p2d], and Xe core was replaced by the effective core potential.[30] For oxygen and nitrogen, we used the standard LANL2DZ plus diffuse and polarization functions.[31] On the other hand, for the calculations of the core electron binding energy of the adsorbed NO using the

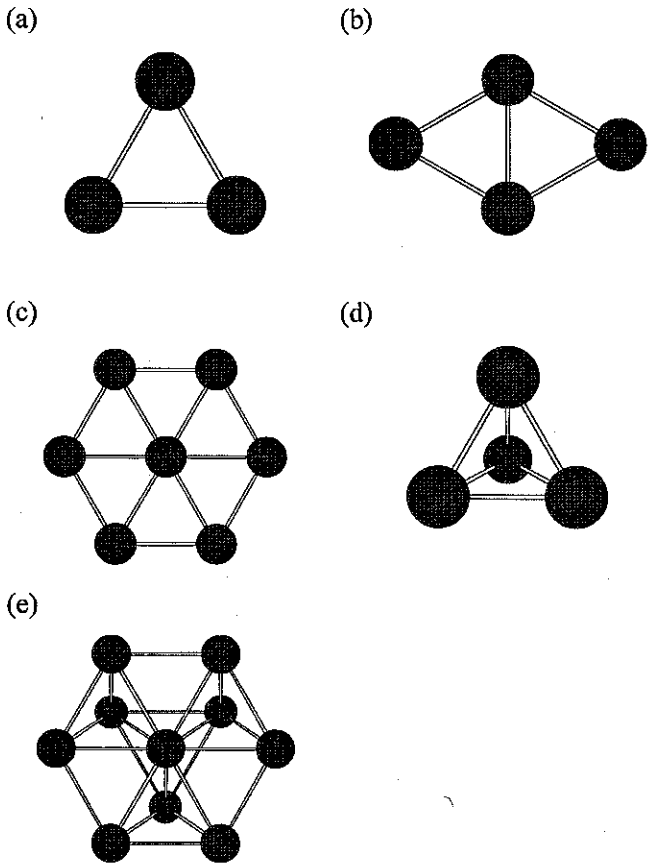

Figure 2. Cluster models used in this work: (a) $Pt_3(3,0)$, (b) $Pt_4(4,0)$, (c) $Pt_7(7,0)$, (d) $Pt_4(3,1)$, and (e) $Pt_{10}(7,3)$.

SAC-CI general-*R* method, we used the basis set well tested in the correlation calculations. We used the Ahlrich's core-valence triple-ζ basis[32] for N and O atoms and Christiansen's ECP basis for Pt.[33] The reference functions for the SAC-CI calculations were the Hartree–Fock wave function chosen for the DAM.

3. DAM vs CM

Table 1 shows a comparison between the DAM and CM for the adsorption energy and the charges of NO on the Pt(111) surface. The adsorption geometries were optimized independently for both CM and DAM. Referring to the adsorption energy, we see that the CM does not describe a stable adsorption of NO on the Pt(111) surface. The adsorption energy calculated by the CM is negative for all the adsorption sites, while the DAM gives positive (stable) adsorption energy for all the adsorption sites. This clearly shows the advantage of the DAM over the CM, since experimentally NO is preferably adsorbed on the Pt(111) surface. Furthermore, the stability order is also in contradiction with that of DAM and the experiment (as seen later): the 3-fold site is more repulsive than the on-top site. Detailed discussions on the relative stabilities, etc., will be given below.

We show in Table 2 the size dependence of the adsorption energy in the DAM and CM. Not only for the $Pt_{10}(7,3)$ model given in Table 1, the CM gives negative adsorption energy in various cases, while the DAM gives always the positive adsorption energy. The cluster size dependence in the DAM will be discussed in the next section.

We see that the DAM describes larger electron transfer to NO than the CM. The NO charge calculated with the DAM is -0.4 for the 3-fold site, -0.1 for the 2-fold site, and -0.14 for the on-top site, while that with the CM is -0.24, $+0.03$, and 0.0, respectively. This electron transfer from the Pt surface to the π^* orbital of NO seems to be important for describing the interaction between the chemisorbed NO on a metal surface.

We show in Table 1 the calculated stretching vibration frequency of NO (ν_{NO}) and the IR intensity both with the DAM and CM. As we will see from discussions given below, the DAM gives reasonable vibration frequency for both 3-fold and on-top geometries, but the frequency calculated with the CM is not well comparable with the experimental values.

The IR peak intensity of the higher frequency (1700–1725 cm^{-1}) is larger than lower one (1476–1516 cm^{-1}).[16] This means that the IR intensity is larger at the on-top site than at the 3-fold site. This is reproduced with the DAM but not with the CM.

The above comparative calculations show that the electron transfer from the bulk metal to the adsorbates is important for the adsorption of NO on the Pt surface. Then we use the DAM to study the chemisorption and spectroscopy of NO on the Pt(111) surface.

4. Structure, Vibrational Frequency, and Adsorption Energy – Cluster Size Dependence

The structure of NO on the Pt(111) surface was observed by spectroscopic techniques such as NEXAFS.[12] Two types of NO adsorbates with the bond lengths of 1.16 and 1.24 Å[12] were reported on the Pt(111) surface. Croci et al. reported experimentally the adsorption energy of NO on the Pt(111) surface to be 1.29 eV.[8] Only one adsorption energy was reported, and this energy seems to correspond to the most stable adsorption species of NO on the Pt(111) surface. This adsorption energy on the Pt(111) surface is smaller than those on other indices of the Pt surface reported by Yeo, Vattuone, and King, namely 1.98 eV on Pt(100)[34] and 1.68 eV on Pt(110),[35] representing the natures of the interactions between the surfaces and the adsorbates.

We examined here first the cluster size dependence of the DAM on the optimized geometry, vibrational frequency, and the adsorption energy by using five different types of clusters shown in Figure 2. The result of the calculation was summarized in Table 3. We see first small model size dependence on the optimized NO length. For the on-top site, the calculated length was 1.19, 1.19, 1.20, 1.17, and 1.20 Å for the $Pt_3(3,0)$, $Pt_4(4,0)$, $Pt_7(7,0)$, $Pt_4(3,1)$, and $Pt_{10}(7,3)$ models, respectively. This result indicates that the experimental bond length of 1.16 Å[12] would correspond to the on-top type NO. Similarly, we also examined the NO length for other adsorption sites, 2-fold bridge, 3-fold fcc hollow, and 3-fold hcp hollow sites. The calculated NO length for the 2-fold bridge site was in the range of 1.20–1.21 Å and that of the 3-fold hollow fcc and hcp sites was in the range of 1.22–1.24 Å. The experimentally proposed value for the bridge or hollow site was 1.24 Å.[12] From the present result,

Table 1. Adsorption Energies (E_{ads}) and Charges of $Pt_{10}(7,3)$ Model: Comparison of the DAM and the Neutral Cluster Model

site model		on-top		2-fold		3-fold fcc		3-fold hcp	
		DAM	CM	DAM	CM	DAM	CM	DAM	CM
E_{ads} (eV)	calc	0.37	−1.41	0.50	−1.31	1.25	−1.53	1.26	−1.60
	exptl.						1.29		
ν_{NO} (cm^{-1})	calc	1706	1752	1626	1689	1482	1536	1475	1484
	exptl.	1700−1725					1476−1516		
IR intensity		639	432	522	496	396	362	497	492
charge on N		−0.12	−0.03	−0.09	−0.01	−0.21	−0.11	−0.20	−0.11
charge on O		−0.02	0.03	−0.01	0.04	−0.19	−0.13	−0.22	−0.12
charge on Pt[a]		0.57	1.00	0.21	0.37	0.10	0.18	0.17	0.12

[a] The averaged value for the nearest Pt atoms from NO adsorbate.

Table 2. Size Dependencies in the DAM and the CM on the Adsorption Energy ($E_{ads.}$) in eV Using Five Clusters Shown in Figure 2

site model	on-top		2-fold		3-fold fcc		3-fold hcp	
	DAM	CM	DAM	CM	DAM	CM	DAM	CM
Pt_3 (3,0)	2.09	0.22	1.49	−0.50	1.89	−0.21		
Pt_4 (4,0)	1.90	−0.57	1.59	−1.19	2.71	−0.15		
Pt_4 (3,1)	1.24	−0.73	1.23	−1.03			1.43	−0.83
Pt_7 (7,0)	1.70	0.60	2.02	−0.02	2.94	0.24		
Pt_{10} (7,3)	0.37	−1.41	0.50	−1.31	1.25	−1.53	1.26	−1.60
exptl.[a]					1.29			

[a] Reference 8.

Table 3. Cluster Size Dependences of the DAM on the Calculated NO Length, Frequency, and the Adsorption Energy ($E_{ads.}$) Using Five Clusters Shown in Figure 2

site	model	R_{N-O} (Å)	ν_{N-O} (cm^{-1})	E_{ads} (eV)
on-top	Pt_3 (3,0)	1.19	1661	2.09
	Pt_4 (4,0)	1.19	1690	1.90
	Pt_4 (3,1)	1.20	1666	1.24
	Pt_7 (7,0)	1.17	1762	1.70
	Pt_{10} (7,3)	1.18	1706	0.37
2-fold	Pt_3 (3,0)	1.21	1503	1.49
	Pt_4 (4,0)	1.21	1594	1.59
	Pt_4 (3,1)	1.21	1572	1.23
	Pt_7 (7,0)	1.20	1648	2.02
	Pt_{10} (7,3)	1.20	1626	0.50
3-fold fcc-hollow	Pt_3 (3,0)	1.24	1406	1.89
	Pt_4 (4,0)	1.24	1442	2.71
	Pt_7 (7,0)	1.22	1503	2.94
	Pt_{10} (7,3)	1.23	1482	1.25
3-fold hcp-hollow	Pt_4 (3,1)	1.23	1453	1.43
	Pt_{10} (7,3)	1.23	1475	1.26
exptl.		1.16[b]	1700−1725[a]	1.29[c]
		1.24[b]	1476−1516[a]	

[a] Reference 16. [b] Reference 12. [c] Reference 8.

we assigned the observed bond length of 1.24 Å to be due to the 3-fold hollow site. Thus, the small cluster size dependence of the calculated NO length and the reliability of the present DAM model have enabled us to make a unique assignment of the adsorption site.

We next calculated the NO vibration frequency at the optimized geometry of the different size DAM. The calculated N−O stretching frequency for the on-top site was in the range of 1661−1762 cm^{-1}, that for the 2-fold site was 1503−1648 cm^{-1}, and that for the 3-fold hollow site was 1406−1503 cm^{-1}. Two different stretching frequencies were reported by EELS and IRAS,[16] which would correspond to different absorption species of NO on the Pt(111) surface. The lower frequency was 1476−1516 cm^{-1} and the higher one was 1700−1725 cm^{-1}. Compared to our theoretical results, the stretching band of the lower frequency is assigned to the NO on the 3-fold hollow site and that of higher frequency is assigned to the on-top one.

Finally, we examine the adsorption energy ($E_{ads.}$), which is defined as the stabilization energy of NO adsorbed on the surface relative to the gas-phase; $E_{ads.} = E(Pt_n) + E(NO) - E(Pt_nNO)$. The calculated adsorption energy shows a relatively large model size dependence and a small size DAM tends to overestimate the adsorption energy. This is because the small cluster has a relatively large number of unsaturated bonds that are stabilized by forming Pt_nNO. The result of the largest DAM using $Pt_{10}(7,3)$ cluster is 1.25 eV for the 3-fold fcc-hollow site and 1.26 eV for the hcp-hollow site, in good agreement with the experimental value, 1.29 eV. This indicates that the experimental value is due to the adsorption on the 3-fold hollow site. The comparison with the $Pt_7(7,0)$ model for the 3-fold fcc-hollow site clearly shows an important role of the second Pt layer in the $Pt_{10}(7,3)$ cluster.

5. Geometry and Potential Energy Diagram of NO on the Surface

We examined the potential energy diagram of NO on the Pt(111) surface using the Pt_{10} (7,3) model and showed the result in Figure 3. The values in parentheses are the results obtained with the $Pt_7(7,0)$ model. The potential energy (E_p) is defined similarly to the adsorption energy as $E_p = E(Pt_n) + E(NO) - E(Pt_nNO)$ and is a function of the position of NO on the surface. We also show in Figure 3 the optimized geometries (RC1−RC3) and the transition states (TS1, TS2). The energy difference between the 3-fold fcc and hcp hollow sites was very small, only 0.01 eV, and therefore, we use in the following discussions the result of the 3-fold fcc hollow site model. For the migrating from the on-top site to the 3-fold site, the transition state (TS1) was found and the barrier was 0.59 eV. We also found another TS (TS2) from the on-top site to the 2-fold site and the barrier was 0.22 eV. The on-top site (RC1) and the 3-fold hollow site (RC3) had true minima, but there was no true minimum at the 2-fold bridge site: it was a transient species that is not stable. This

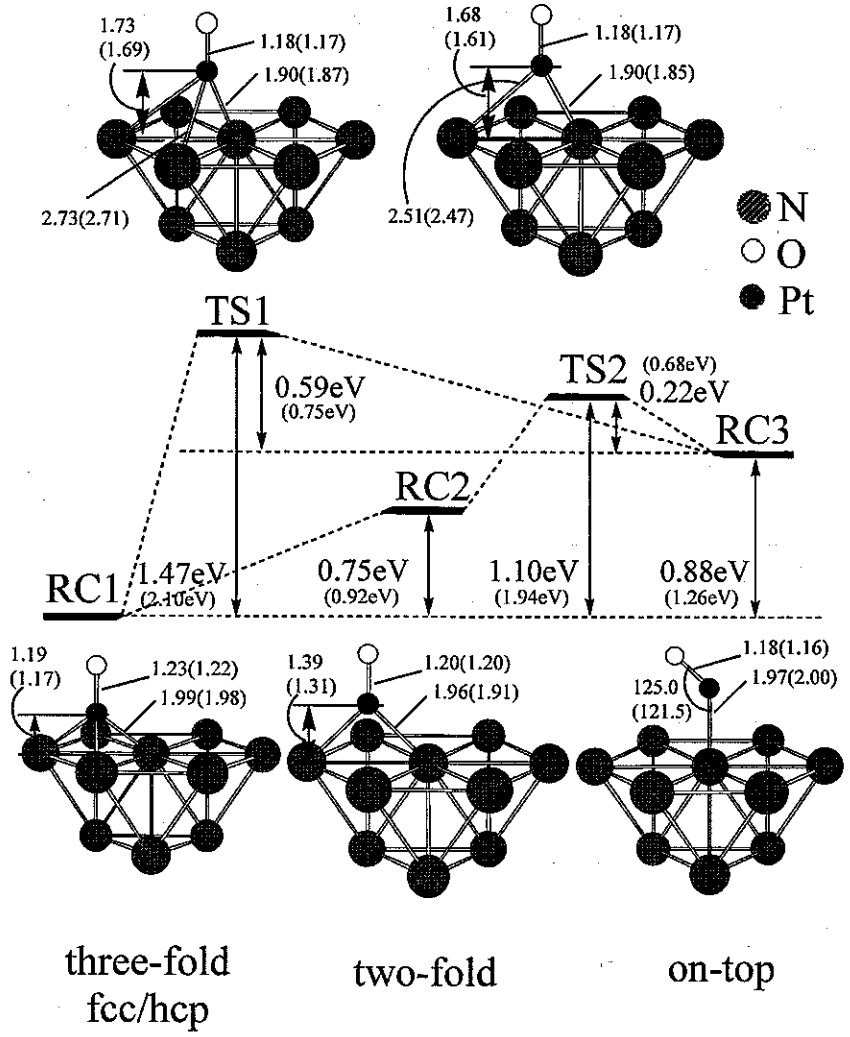

Figure 3. Potential energy diagram and the geometries of the NO adsorbates on the $Pt_{10}(7,3)$ DAM. Values in parentheses are due to $Pt_7(7,0)$ DAM.

result indicates that, at low coverage, the NO adsorbed on the on-top site migrates to the most stable 3-fold site via the 2-fold site. The NO at the 3-fold (fcc or hcp) hollow site is strongly bound with a relatively high barrier of about 0.75 eV for the migration to another 3-fold (hcp or fcc) hollow site and therefore would not easily move to the other sites at low temperature.

Next, we examined the Pt−N−O angle at the on-top site using the $Pt_{10}(7,3)$ DAM. At each Pt−N−O angle, the Pt−N and N−O lengths were optimized. The adsorption energy of the linear form (180 degree) was −2.24 eV and of the bent form (121.7 degree) was 1.49 eV, which was the local minimum. Namely, at the on-top site, NO takes a bent form with the Pt−N−O angle of around 120 degrees. Similar calculations were also done at the 3-fold fcc hollow site. There, the adsorption energy of the linear form was 2.81 eV and that of the bent form was −0.20 eV. So, a linear form is preferred at this site. In summary, the two adsorption species are linear NO at the 3-fold fcc hollow site and the bent NO at the on-top site.

In Table 4, our theoretical results are compared with those of other experimental and theoretical studies on the on-top and the 3-fold hollow sites. When we use the $Pt_{10}(7,3)$ model, there was no apparent difference between the fcc and hcp sites. The experimental adsorption energy on Pt(111) was 1.29 eV,[8] while the calculated adsorption energy was 0.37 eV for the on-top site and 1.25 eV for the 3-fold hollow site. So, the measured adsorbate would be NO on the 3-fold hollow site. The adsorption energies of the other index Pt(100)[34] and Pt(110)[35] were reported to be 1.98 and 1.68 eV, respectively. These differences reflect the nature of the interaction between NO and the surface.

Table 4. Comparison of the Present and Past Results on the Adsorption Energy of NO on the Pt Surfaces

		present DAM+B3LYP for Pt(111)[a]	other theoretical works	exptl.
on-top		0.37	0.64[c], 1.61[b]	
3-fold	fcc-hollow	1.25	1.75[c], 2.09[b]	1.29 [Pt(111)][d]
	hcp-hollow	1.25	1.92[b]	1.68 [Pt(100)][e]
				1.98 [Pt(110)] [f]

[a] $Pt_{10}(7,3)$ DAM. [b] Reference 19. [c] Reference 17. [d] Reference 8. [e] Reference 33. [f] Reference 32.

6. Vibrational Analysis

In a gas phase, the N−O length is 1.15077 Å and the vibrational frequency is 1876 cm^{-1}.[36] The corresponding

Table 5. Bond Length and Stretching Frequency of NO on the Pt(111) Surface and Atomic Charge of Each Atom

adsorption site		R_{N-O} (Å)	ν_{N-O} (cm^{-1})	atomic charge N	atomic charge O
on-top		1.18	1706	−0.12	−0.02
3-fold	fcc-hollow	1.23	1482	−0.19	−0.21
	hcp-hollow	1.23	1475	−0.20	−0.22
		1.16[b]	1476−1516[a]		
exptl.		1.24[b]	1700−1725[a]		

[a] Reference 16. [b] Reference 12.

values on the Pt(111) surface calculated with the $Pt_{10}(7,3)$ DAM are summarized in Table 5 together with the Mulliken charges on N and O atom. In the EELS experiment, the peak developed in 1476−1516 cm^{-1} appears first at low coverage and at higher coverage a second new peak appears at around 1700 cm^{-1} and the first peak is replaced with the second peak as the coverage is further increased. The present result shown in Table 5 clearly assigns the first peak as being due to the NO at the stable 3-fold hollow site and the second peak as being due to the on-top NO. Further, the experimental bond lengths of 1.24 and 1.16 Å due to Esch et al.[12] are also clearly assigned as being due to the NO's at the 3-fold hollow site and at the on-top site, respectively.

The dipole moment of the adsorbed NO on the 3-fold site was smaller than that of the on-top site, so that the vibrational peak intensity of the 3-fold site would be smaller than that of the on-top site, in agreement with the experimental spectrum.[2] We show in Figure 4 the theoretical and experimental vibrational spectra[2] of NO/Pt(111). The ratio of the adsorption molecules was assumed to be 1:1:1 (on-top:3-fold fcc:3-fold hcp) in the theoretical spectrum. The theoretical spectrum agrees well with the experimental one taken at the 0.50 ML coverage.

7. K-Shell Ionization Potential

Core electron binding energies (CEBEs) and the chemical shifts of the adsorbates are important information of analytical chemistry for surface adsorbates. We can calculate the CEBEs of various molecules in high accuracy using the SAC/SAC-CI general-*R* method.[24,37−39] The orbital reorganization due to the core−electron ionization is described by the general-*R* method together with the important correlation effect. Here, we apply this established method to the calculations of the N 1s and O 1s CEBEs of the NO molecule adsorbed on the Pt(111) surface. In this calculation we used Ahlrich's core-valence triple-ζ basis[32] set for N and O atoms

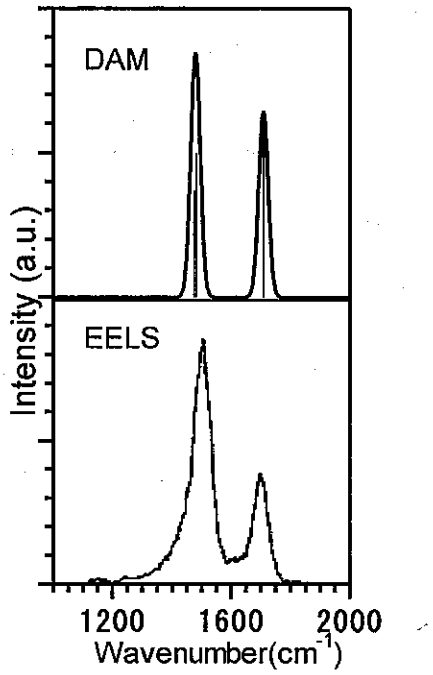

Figure 4. Theoretical vs experimental vibrational spectrum of NO/Pt(111). The experimental spectrum was cited from the 0.25 L exposure data of NO by Gland et al. (Figure 1 of ref 2).

and Christiansen's ECP for Pt atom.[33] These basis sets are well examined for the SAC-CI calculations of the K-shell ionization potential.[24,37−39]

The results of the calculations were shown in Table 6. The CEBEs of a free NO molecule were calculated to be 411.1 and 543.1 eV for N and O atoms, respectively, which were in good agreement with the experimental values, 410.8 and 543.6 eV,[40] respectively. For the NO adsorbed at the on-top, fcc-hollow, and hcp-hollow sites, the calculated O 1s CEBEs were 538.5, 537.5, and 537.2 eV, respectively. The experimental CEBEs are estimated to be 538.9 and 537.0 eV[4] using the work function $\phi = 6.42$ eV,[41] and so the band of higher energy was assigned to the on-top site and the lower one to the fcc/hcp-hollow site. The theoretical energy difference from the free molecule to the adsorbate is 5.1, 6.1, and 6.4 eV, respectively, for the on-top, fcc-hollow, and hcp-follow sites, which were proportional to the atomic charges, −0.02 (on-top), −0.21 (fcc-hollow), and −0.22 (hcp-hollow), which were also shown in Table 5.

The theoretical values of N 1s CEBEs were 406.3, 407.4, and 407.6 eV for the on-top, fcc- and, hcp-hollow sites,

Table 6. Core Electron Binding Energies and Atomic Charges of Free and Adsorbed NO

state		N 1s exptl. (eV)	N 1s DAM+SAC-CI IP (eV)	N 1s DAM+SAC-CI charge on N	O 1s exptl. (eV)	O 1s DAM+SAC-CI IP (eV)	O 1s DAM+SAC-CI charge on O
on-top		407.0[a]	406.3	0.07	538.9[a]	538.5	−0.24
2-fold bridge			405.8	0.02		538.7	−0.18
3-fold	fcc-hollow		407.4	0.09		537.0[a]	537.5
	hcp-hollow		407.6	0.10		537.2	−0.38
gas phase		410.8[b]	411.1	0.15	543.6[b]	543.2	−0.15

[a] Reference 4. [b] Reference 38.

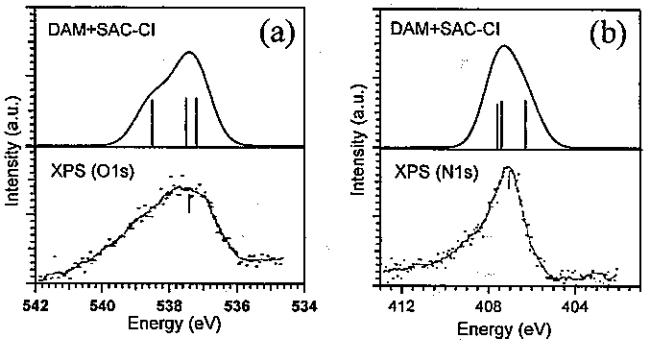

Figure 5. DAM+SAC-CI theoretical vs experimental photoemission spectrum of NO/Pt(111): (a) O 1s hole spectrum and (b) N 1s hole spectrum. The experimental spectra was observed by Kiskinova et al. (Figure 3 of ref 4).

respectively, and the experimental value was only 407.0 eV[4], which was near the average value of our results, 407.1 eV. We show the theoretical and experimental CEBE spectra of NO/Pt(111) in Figure 5. The ratio of the adsorbates was assumed to be 1:1:1 (on-top: 3-fold fcc: 3-fold hcp) in calculating the theoretical spectrum, which corresponds to the experimental condition of the higher or saturated coverage.

8. NO−NO Interaction at High Coverage

We examine here the NO−NO interaction that is expected in high coverage. For the on-top adsorption, the former model (one NO molecule on the surface) may not have been appropriate since it appears only at a high coverage situation. Therefore, we examine $Pt_x(NO)_2$ (x=10,11,12) DAM shown in Figure 6 for the high coverage model. When two NO molecules are put in the p(2 × 2) unit cell at the coverage of 0.50 ML, we assume that one is the on-top site and another is the 3-fold site (model (b) and (c)), referring to the experimental LEED pattern[15] and STM image.[13,14] We also examined the interaction between the NO's on the 3-fold fcc and hcp sites (model (a)). The calculation method and the basis sets are the same as before.

Table 7 shows the results, which should be compared with the single NO results shown in Table 5. There were little interactions between the on-top site and the 3-fold fcc or hcp hollow sites. The NO distances were completely the same, and the frequencies were shifted only slightly. On the other hand, a small interaction was found between the fcc and the hcp hollow sites and the theoretical spectrum was split into two peaks, 1430 and 1485 cm^{-1}. We assume that the vibrational spectrum in the region of 1400−1500 cm^{-1} becomes broad at high coverage by such an interaction between the adsorbates.

9. Conclusion

The DAM has been applied to the NO on the Pt(111) surface. The spectroscopic properties such as the adsorption energy, the geometry and the vibrational frequency of the NO adsorbates were theoretically calculated and compared with the experimentally available data. We also calculated the potential energy surface of the NO adsorbate on the Pt(111) surface. We could show that only the 3-hold hollow site (fcc and hcp) and the on-top site are stable. We gave a definite assignment of the observed spectra and clarified the nature and the electronic structure of the adsorbate on the Pt(111) surface.

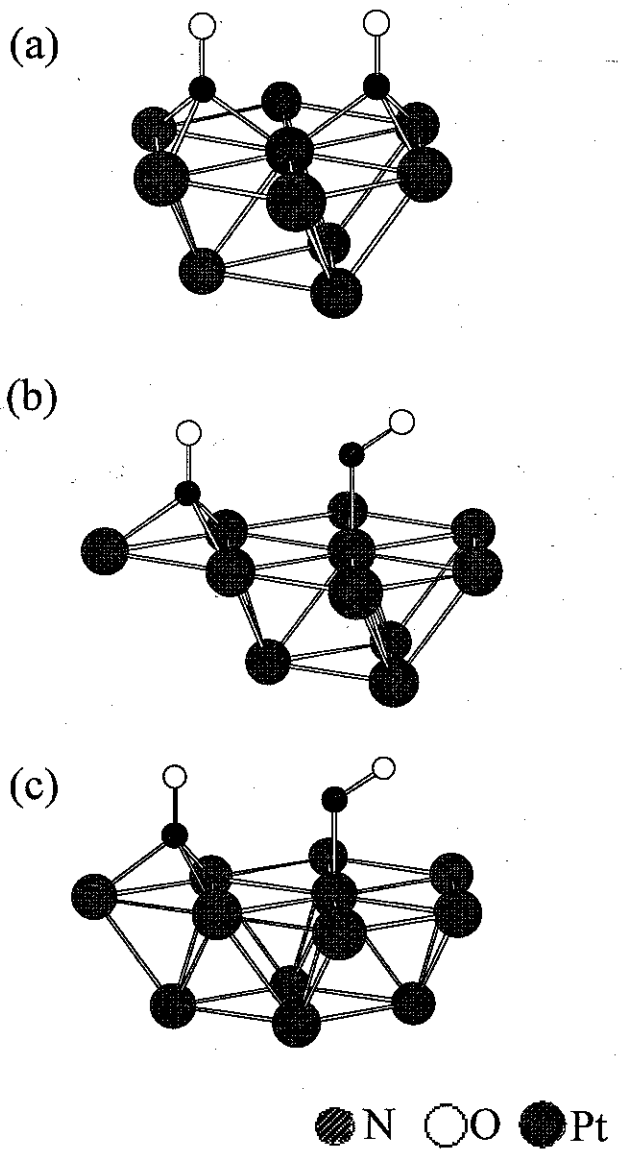

Figure 6. Optimized geometries of NO of $Pt_x(NO)_2$ [x = 10−12]: (a) fcc and hcp-hollow, (b) on-top and fcc-hollow, and (c) on-top and hcp-hollow.

Table 7. Bond Length and Frequency of Adsorbed NO and Atomic Charge of Each Atom: (a) the fcc and hcp-hollow Model, (b) the on-top and fcc-hollow Model, and (c) the on-top and hcp-hollow Model

model	R_{N-O} (Å)	ν_{N-O} (cm^{-1})	atomic charge N	atomic charge O
(a) fcc-hollow + hcp-hollow	1.23	1430	−0.12	−0.25
	1.23	1485	−0.17	−0.25
(b) on-top + fcc-hollow	1.18	1708	−0.08	−0.01
	1.23	1457	−0.27	−0.20
(c) on-top + hcp-hollow	1.18	1707	−0.04	−0.01
	1.23	1468	−0.23	−0.20
exptl.	1.16[a]	1700−1725[b]		
	1.24[a]	1476−1516[b]		

[a] Reference 12. [b] Reference 16.

The dependence on the cluster size used in the DAM was examined for the adsorption energy, the geometry and the vibrational frequency. The dependence was relatively large for the adsorption energy but small for the geometry and the vibrational frequency. Anyway, the largest model examined has given the results that agree best with the experimental values. Generally speaking, it is rather difficult to eliminate the edge effects of the model, but comparing with the experimental values, this effect seems to be minimized by using the largest adcluster model.

The inner-core electron binding energy of NO on the Pt surface was calculated by the SAC-CI general-R method using the MO's obtained with the DAM. Likewise the gas-phase case, the calculated results reproduced well the existing experimental values and predicted the values for nonexisting cases. Since the ESCA spectroscopy is frequently done for surface adsorbates, the SAC-CI + DAM method will provide a powerful method for identifying the surface species.

A comparison of the cluster model (CM) result with the DAM result has clearly shown the importance of the DAM for the adsorbates on a metal surface. These results may be considered as proof of the validity of the DAM.

In conclusion, by combining the experimental and theoretical surface spectroscopies, we can understand the chemistry of the surface adsorbates more deeply than doing only by one of them.

Acknowledgment. This study was supported by a Grant for Creative Scientific Research from the Ministry of Education, Science, Culture, and Sports of Japan and ITBL (IT-based laboratory project) of Japan.

References

(1) Ibach, H.; Lehwald, S. *Surf. Sci.* **1978**, *76*, 1−12.

(2) Gland, J. L.; Sexton, B. A. *Surf. Sci.* **1980**, *94*, 355−368.

(3) Hayden, B. E. *Surf. Sci.* **1983**, *131*, 419−432.

(4) Kiskinova, M.; Pirug, G.; Bonzel, H. P. *Surf. Sci.* **1984**, *136*, 285−295.

(5) Seebauer, E. G.; Kong, A. C. F.; Schmidt, L. D. *Surf. Sci.* **1986**, *176*, 134−156.

(6) Bartram, M. E.; Koel, B. E. *Surf. Sci.* **1989**, *219*, 467−489.

(7) Agrawal, V. K.; Trenary, M. *Surf. Sci.* **1991**, *259*, 116−128.

(8) Croci, M.; Felix, C.; Vandoni, G.; Harbich, W.; Monot, R. *Surf. Sci.* **1994**, *307−309*, 460−464.

(9) Song, M. B.; Suguri, M.; Fukutani, K.; Komori, F.; Murata, Y. *Appl. Surf. Sci.* **1994**, *79/80*, 25−33.

(10) Materer, N.; Barbieri, A.; Gardin, D.; Starke, U.; Batteas, J. D.; Van Hove, M. A.; Somorjai, G. A. *Surf. Sci.* **1994**, *303*, 319−332.

(11) Yoshinobu, J.; Kawai, M. *Chem. Lett.* **1995**, *1995*, 605−606.

(12) Esch, F.; Greber, Th.; Kennou, S.; Siokou, A.; Ladas, S. *Catal. Lett.* **1996**, *38*, 165−170.

(13) Matsumoto, M.; Tatsumi, N.; Fukutani, K.; Okano, T.; Yamada, T.; Miyake, K.; Hate, K.; Shigekawa, H. *J. Vac. Sci. Technol. A* **1999**, *17(4)*, 1577−1580.

(14) Matsumoto, M.; Fukutani, K.; Okano, T.; Miyake, K.; Shigekawa, H.; Kato, H.; Okuyama, H.; Kawai, M. *Surf. Sci.* **2000**, *454−456*, 101−105.

(15) Matsumoto, M.; Tatsumi, N.; Fukutani, K.; Okano, T. *Surf. Sci.* **2002**, *513*, 485−500.

(16) Garin, F. *Appl. Catal. A* **2001**, *222*, 183-219.

(17) Ge, Q.; King, D. A. *Chem. Phys. Lett.* **1998**, *285*, 15−20.

(18) Koper, M. T. M.; van Santen, R. A.; Wasileski, S. A.; Weaver, M. J. *J. Chem. Phys.* **2000**, *113(10)*, 4392−4407.

(19) Aizawa, H.; Morikawa, Y.; Tsuneyuki, S.; Fukutani, K.; Ohno, T. *Surf. Sci.* **2002**, *514*, 394−403.

(20) Nakatsuji, H. *J. Chem. Phys.* **1987**, *87(8)*, 4995−5001.

(21) Nakatsuji, H. *Prog. Surf. Sci.* **1997**, *54(1)*, 1−68.

(22) Nakatsuji, H.; Hirao, K. *J. Chem. Phys.* **1978**, *68*, 2053−2065.

(23) (a) Nakatsuji, H. *Chem. Phys. Lett.* **1978**, *59*, 362−364. (b) Nakatsuji, H. *Chem. Phys. Lett.* **1979**, *67*, 329−333, 334−342.

(24) (a) Kuramoto, K.; Ehara, M.; Nakatsuji, H. submitted for publication. (b) Kuramoto, K.; Ehara, M.; Nakatsuji, H.; Kitajima, M.; Tanaka, H.; Fanis, A. D.; Tanemori, Y.; Ueda, K. *J. Electron Spectrosc. Relat. Phenom.* **2004**, in press.

(25) Becke, A. D. *J. Chem. Phys.* **1993**, *98*, 5648−5652.

(26) Lee, C.; Yang, W.; Parr, R. G. *Phys. Rev. B* **1988**, *37*, 785−789.

(27) Nakatsuji, H.; Nakai, H.; Fukunishi, Y. *J. Chem. Phys.* **1991**, *95(1)*, 640−647.

(28) Sutton, L. E. *Tables of Interatomic Distances and Configuration in Molecules and Ions;* Royal Society of Chemistry: London, 1965.

(29) Gaussian 03, M. J. Frisch, G. W. Trucks, H. B. Schlegel, G. E. Scuseria, M. A. Robb, J. R. Cheeseman, J. A. Montgomery, Jr., T. Vreven, K. N. Kudin, J. C. Burant, J. M. Millam, S. S. Iyengar, J. Tomasi, V. Barone, B. Mennucci, M. Cossi, G. Scalmani, N. Rega, G. A. Petersson, H. Nakatsuji, M. Hada, M. Ehara, K. Toyota, R. Fukuda, J. Hasegawa, M. Ishida, T. Nakajima, Y. Honda, O. Kitao, H. Nakai, M. Klene, X. Li, J. E. Knox, H. P. Hratchian, J. B. Cross, C. Adamo, J. Jaramillo, R. Gomperts, R. E. Stratmann, O. Yazyev, A. J. Austin, R. Cammi, C. Pomelli, J. W. Ochterski, P. Y. Ayala, K. Morokuma, G. A. Voth, P. Salvador, J. J. Dannenberg, V. G. Zakrzewski, S. Dapprich, A. D. Daniels, M. C. Strain, O. Farkas, D. K. Malick, A. D. Rabuck, K. Raghavachari, J. B. Foresman, J. V. Ortiz, Q. Cui, A. G. Baboul, S. Clifford, J. Cioslowski, B. B. Stefanov, G. Liu, A. Liashenko, P. Piskorz, I. Komaromi, R. L. Martin, D. J. Fox, T. Keith, M. A. Al-Laham, C. Y. Peng, A. Nanayakkara, M. Challacombe, P. M. W. Gill, B. Johnson, W. Chen, M. W. Wong, C. Gonzalez, and J. A. Pople, Gaussian, Inc., Pittsburgh, PA, 2003.

(30) Hay, P. J.; Wadt, W. R. *J. Chem. Phys.* **1985**, *82*, 270−283.

(31) Check, C. E.; Faust, T. O.; Bailey, J. M.; Wright, B. J.; Gilbert, T. M.; Sunderlin, L. S. *J. Phys. Chem. A* **2001**, *105*, 8111−8116.

(32) Schafer, A.; Horn, H.; Ahlrichs, R. *J. Chem. Phys.* **1992**, *97*, 2571−2577.

(33) Ross, R. B.; Ermler, W. C.; Christiansen, P. A. *J. Chem. Phys.* **1990**, *93*, 6654−6670.

(34) Yeo, Y. Y.; Vattuone, L.; King, D. A. *J. Chem. Phys.* **1997**, *106*, 1990−1996.

(35) Yeo, Y. Y.; Vattuone, L.; King, D. A. *J. Chem. Phys.* **1996**, *104*, 3810−3821.

(36) Huber, K. P.; Herzberg, G. *Molecular Spectra and Molecular Structure, IV. Constant of Diatomic Molecules*; Van Nostrand: Princeton, NJ, 1979.

(37) Nakatsuji, H. *Chem. Phys. Lett.* **1991**, *177*, 331−337.

(38) Nakatsuji, H. *J. Chem. Phys.* **1985**, *83*, 713−722.

(39) Nakatsuji, H. *J. Chem. Phys.* **1985**, *83*, 5743−5748.

(40) Bakke, A. A.; Chen, A. W.; Jolly, W. L. *J. Electron Spectrosc.* **1980**, *20*, 333−366.

(41) Wandelt, K. *Chemistry and Physics of Solid Surface VII*; Springer: 1990; p 289.

CT049938Z